Published: Semiconductors and Rare Earth Based Materials
(World Scientific, Singapore, 1991), pp. 3-17
Presented: International Workshop on Materials Science
Hanoi, Vietnam, October 15-26, 1990

OPTICAL ABSORPTION OF DOPED SEMICONDUCTORS

C.A.J. AMMERLAAN
Natuurkundig Laboratorium der Universiteit van Amsterdam
Valckenierstraat 65, NL-1018 XE Amsterdam
The Netherlands

ABSTRACT

Optical properties of semiconductors at sub-bandgap energies are largely determined by crystal lattice defects and impurities. The present review discusses the relation between dopants and optical spectra by treating examples of a) optical vibrational absorption and b) the detection of magnetic resonance via optical electronic absorption.

1. Introduction

The optical properties of crystalline semiconductors at photon energies below the intrinsic bandgap are greatly influenced by impurities and crystal lattice defects. For an identification and full characterization of the optical centres one needs to determine (a) their concentration, (b) the associated electronic levels determining (c) the donor, acceptor or amphoteric nature and (d) the charge state, (e) the carrier emission and capture cross sections, (f) the chemical identity of the atomic constituents, (g) possible breathing-mode or symmetry-lowering lattice relaxations, establishing (h) the static or dynamic defect symmetry and (i) wavefunctions for the defect electrons. Many experimental methods are available for the investigation of centres. Since specific techniques probe one or some of the aspects mentioned only, the full characterization requires extensive investigation, applying several of the available methods. Optical spectroscopy, either in absorption or emission, mainly characterizes defects by the energies of the spectral lines and the intensities. By magnetic resonance information on atomic structure, hence defect identification, is mainly obtained. To great advantage methods of double spectroscopy, in which the electron and spin transitions are simultaneously induced, can be applied. In this tutorial review examples will be discussed of defect characterization by optical absorption and by the combination of optical and magnetic resonance spectroscopy. The focus will be on the illustration of the relation between the structure of the impurity or defect centre and the resulting optical properties of the semiconductor material.

2. Optical absorption

In the passing of light through matter photons can be lost by the excitation of electrons or the creation of phonons. Such processes can be related to the intrinsic, pure and perfect, semiconductor crystal. Electrons can be excited from occupied valence band states to empty states in conduction bands, yielding strong absorption at energies above the fundamental edge. At energies below the bandgap value transitions involving gap states are dominant. It allows the study of deep or shallow states related to semiconductor dopants. Also for lattice vibrations the effects of localized centres can, under suitable conditions, be distinguished clearly from the host crystal effects. In the undoped crystal the one-phonon energies fall in the range from zero to a maximum energy. Fig. 1 illustrates the phonon frequency spectrum for the simplified case of the one-dimensional crystal with

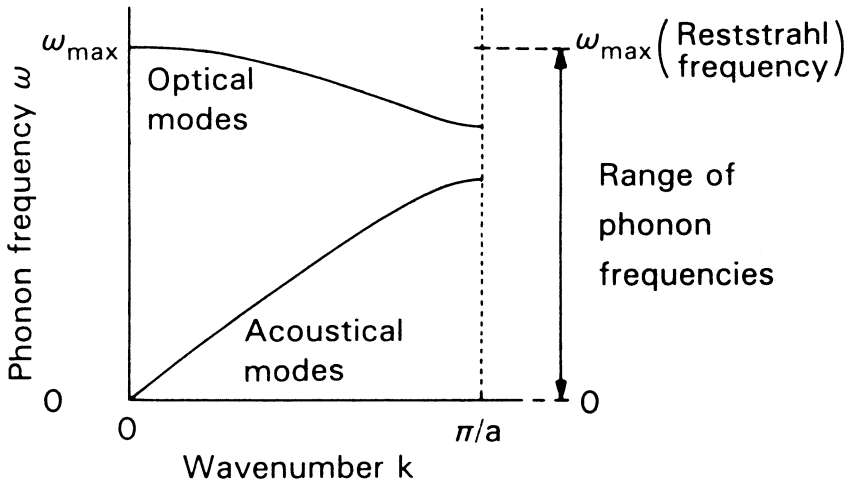

Figure 1 : Phonon spectrum in a two-atomic linear crystal.

lattice parameter a and two atoms in the unit cell. Impurities which are lighter than the atoms of the host give rise to vibrations at higher frequency than the maximum ω_{max} existing in the pure crystal. These vibrations are localized in the vicinity of the impurity site and are hence called local modes. A simple model to analyse these vibrations is given in Fig. 2. On the basis of this model it is easily derived that the local mode frequency is given by:

$$\omega_{loc}^2 = \omega_{max}^2 \frac{M^2}{m(2M-m)} = \frac{\omega_{max}^2}{\mu(2-\mu)} \quad , \tag{1}$$

where μ is the ratio of the light impurity mass m to the heavy crystal atom mass M. A graphical representation of this result is given in Fig. 3.

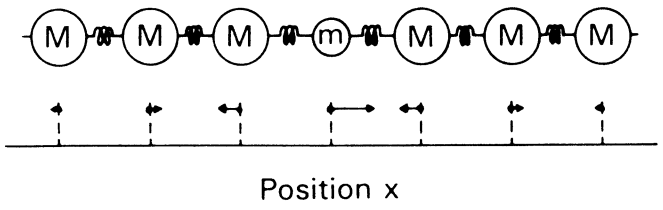

Figure 2 : Linear chain model for local mode vibrations in a mono-atomic crystal.

A classical well-studied case demonstrating the absorption related to local mode vibrations is the hydrogen impurity in alkali-halide crystals. Hydrogen atoms substitute for the halogen ions forming so-called U-centres, of which the atomic structure is schematically illustrated in Fig. 4. The related local mode absorption is shown in Fig. 5. It is found at a wavelength near 20 μm, considerably below the minimum wavelength of about 70 μm reported for the intrinsic crystal vibrations [1,2]. In comparing with the prediction based on equation 1, with m/M $\approx$ 1/37 and $\omega_{loc}/\omega_{max} \approx 4.3$, one concludes that the simple model gives some good agreement and allows for basic understanding of the phenomenon.

Oxygen is a most important impurity in semiconductors, notably in silicon. Its mass is below that of silicon and hence absorptions at high frequencies are observable in the infrared spectrum. In its dissolved form oxygen is incorporated in the silicon crystal occupying positions near the bond-centre sites, as indicated in Fig.6. Unlike the previous example of the alkali-halide U-centre, in this case the force constants of binding the impurity, the Si-O bonds, are different from those in the bulk. The covalent bonding is predominantly with the two nearest neighbour silicon atoms. A model to analyse the modes of vibration therefore considers these three atoms. Besides three modes of rigid translations of the Si-O-Si molecule and three modes of rigid rotations, there exist also three modes of vibration. The nomenclature of these vibrations and their oscillatory patterns are given in Fig.7. Due to the different electronegativity of silicon and oxygen all three modes are optically active. Fig.8 illustrates details over a small wavelength region in which the asymmetric bond stretching mode is found. It was recorded at high resolution for a silicon

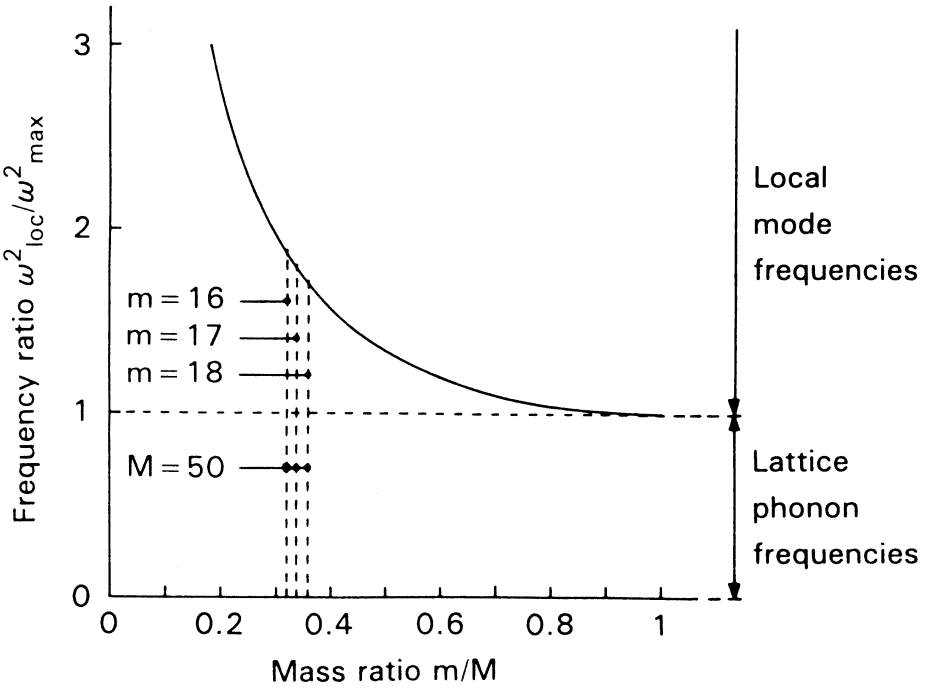

Figure 3 : Local mode frequency as a function of mass ratio, with analysis of the isotopic shifts observed in the asymmetric bond stretching mode of oxygen in silicon.

sample which intentionally was doped with oxygen enriched in the rare isotopes ^{17}O and ^{18}O. In agreement with the basic model the heavier isotopes have the lower vibrational frequency. The isotope effect is, however, quite significantly smaller than expected on the basis of equation 1 using the silicon atom mass 28. The reason for such discrepancy is that the two silicon atoms considered in the model are themselves strongly bonded to the rest of the crystal and are thus restricted in their motion. This greater difficulty to move can be simulated by giving these two atoms a greater effective mass. It appears that an empirical value of effective mass equal to M = 50 allows for a perfect fit of the observed isotope effect. The data points included in Fig.3 illustrate the agreement which can be reached in this empirical treatment. Numerical data related to this analysis are represented in Table 1. The experimentally observed figures are given and the predictions on the basis of the local mode model for the real silicon atom mass M = 28, the effective mass M =

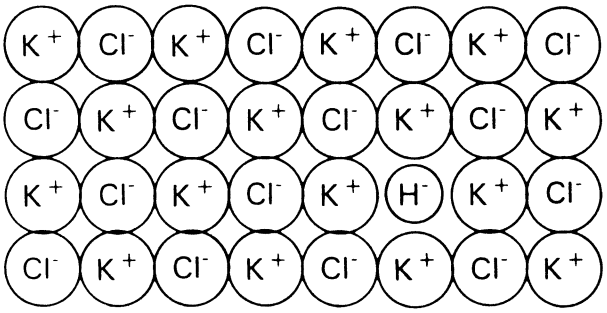

Figure 4 : Structure of the U-centre in KCl:H.

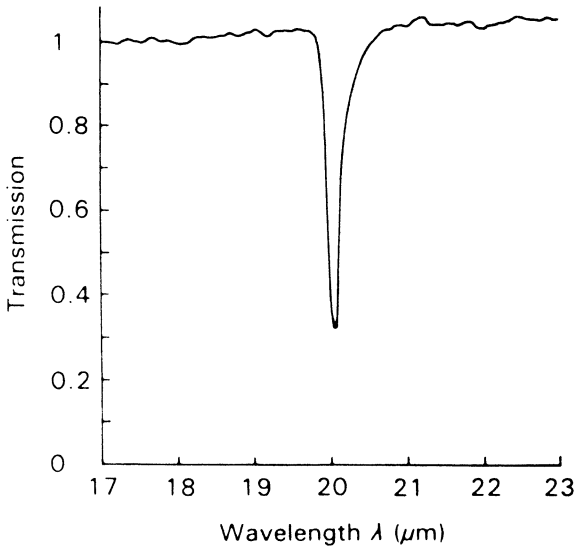

Figure 5 : Local mode absorption of the U-centre in KCl:H, after Schaefer[1].

50 for best fit, and for infinite mass $M = \infty$. In the latter case the square-root law for motion of oxygen in a rigid potential is obtained. Each of the absorption lines of the oxygen isotopes shows further structure related to the presence of silicon isotopes of different mass. Also here the effect of the isotope changes is smaller than expected on the basis of their masses. It again indicates that a larger effective mass must be used to represent reality more closer.

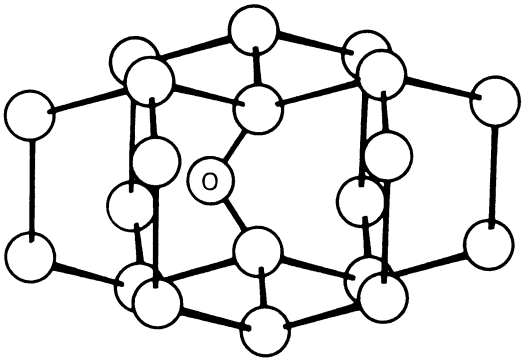

Figure 6 : Structure model of interstitial oxygen in silicon, after Newman and Smith[3].

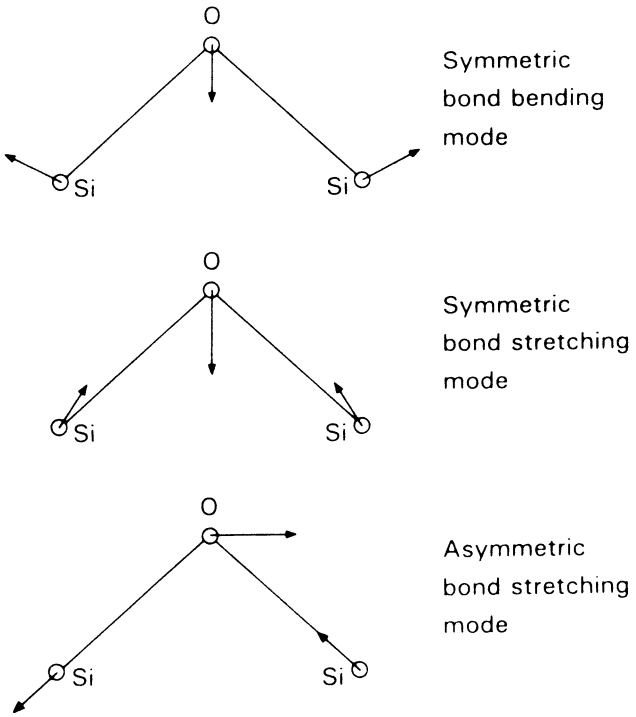

Figure 7 : Normal modes of vibration of the Si-O-Si molecule.

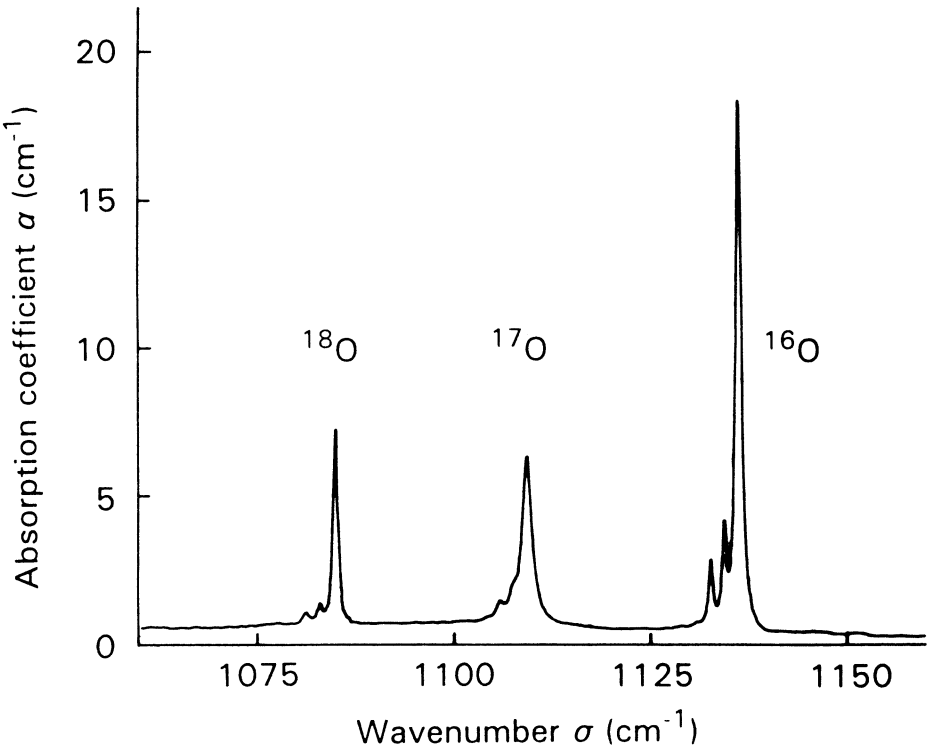

Figure 8 : Isotope effects in the asymmetric bond stretching mode absorption of oxygen in silicon.

Obviously, the simple models as presented can be improved by going to three dimensions, taking more neighbour atoms and force constants into account. The greater complexity then requires more heavy mathematical computation. Examples studied in greater detail include the impurities hydrogen [4,5], boron [6-10] and oxygen [11,12] in silicon. The simple analytical model, however, illustrates basic approaches. These studies contribute to the fundamental scientific knowledge of lattice dynamics. They contribute to materials science by identifying the impurity and affording, once calibration factors are available, the quantitative and selective determination of impurity concentrations.

Table 1 : Isotope effect in the asymmetric bond stretching mode vibration of Si - ^{m}O - Si. Frequencies are given in wavenumber units.

Isotope	σ_{exp} (cm^{-1})	$(\sigma_m/\sigma_{16})_{exp}$	$(\sigma_m/\sigma_{16})_{local\ mode\ model}$		
			M = 28	M = 50	M = ∞
^{16}O	1136	1.000	1.000	1.000	1.000
^{17}O	1109	0.976	0.983	0.976	0.970
^{18}O	1085	0.955	0.967	0.955	0.943

3. Optical detection of magnetic resonance

As mentioned, specific techniques generally reveal only part of the defect properties. The level of information may be improved by resorting to more sophisticated methods of multiple resonance. A prominent example of such strategy employs the linking of magnetic resonance and optical spectra for transitions which have levels in common. The magnetic resonance transition can be an electron paramagnetic resonance (EPR), a nuclear magnetic resonance (NMR) or an electron-nuclear double resonance (ENDOR). By application of such resonance the occupation of levels involved can be changed, the most common practice being the equalization of level populations by saturation of a transition. An optical spin dependent transition involving the same levels will be influenced. The intensity or the degree of polarization of a light absorption or emission can be affected. This affords the optical detection of magnetic resonance (ODMR). Several variations are thus conceivable, as schematically summarized by:

Optical Detection in absorption or emission of
- Electron Paramagnetic Resonance : ODEPR
- Nuclear Magnetic Resonance : ODNMR
- Electron Nuclear Double Resonance : ODENDOR

Combination of the optical and magnetic resonance spectroscopy has several advantageous features. By the conversion of microwave energies typical for the magnetic resonance, ≈ 0.1 meV, to energies of optical photons, ≈ 1 eV, an increase in sensitivity by several orders of magnitude is achieved. In the measurement the defect is characterized by its optical and microwave spectrum jointly, leading to a significant enhancement of selectivity. Both optical and magnetic resonance spectroscopy are distinguished by a high identification power for defects. In rare cases where ambiguity is left by one of the methods, the other spectrum usually eliminates the ambiguity altogether. From the optical part of the experiment energy levels associated with the centre can be positioned with respect to the semiconductor valence or conduction bands. This relates the information on the centre to

its electrical and transport properties. Magnetic resonance commonly reveals the defect symmetry by the anisotropy of the spectra, easily measured normally by angular dependence. Hyperfine interactions are often present and detectable in EPR, or ENDOR, and lead to the atomic identification of the constituents of a centre. On the reverse side, the successful application of a multiple resonance technique requires that all conditions of the resonances can be simultaneously met. The centre must be susceptible to both paramagnetic resonance and optical spectroscopy, restricting the number of suitable systems. Also, generally no sensitivity calibration is available leaving defect concentrations unknown. In evil cases it might happen that an exotic defect ideally satisfies the conditions of sensitivity and selectivity for ODMR, but otherwise manifests itself as a defect with low concentration having minor effect on semiconductor properties.

3.1. ODEPR Absorption Spectroscopy

The basic concepts as applied in absorption ODEPR are illustrated in Fig.9. An optical absorption with an energy typically near 1 eV is the result of an electronic excitation (Fig. 9(a)). The relatively narrow absorption is supposed to be superposed on a background absorption due to external unrelated causes. It is assumed that both ground and excited state in the optical process are paramagnetic with, for ease of illustration, S = 1/2. A magnetic field will split the levels by the Zeeman energy. This splitting is often small compared to the natural linewidth in the optical transitions and remains unobserved. For light propagating in the direction of the magnetic field transitions as indicated in Fig. 9(b) will selectively be induced by circularly polarized light. Experimentally these two components σ_+ and σ_- can be measured separately. Due to higher occupation of the ground state level with $m_s = +1/2$ the component σ_- will have the higher intensity. The different absorption of circularly polarized light in the direction of the magnetic field is called magnetic circular dichroism (MCD). Application of resonant microwave energy in the ground state reduces the population difference $n_+ - n_-$. For full saturation $n_+ = n_-$ and the MCD will completely vanish (Fig. 9(c)). The microwave (magnetic resonance) induced reduction of magnetic circular dichroism has led to an optical effect. Both parts of the spectroscopical investigation are inherently linked as they involve the same electronic levels. While staying on the magnetic resonance and recording the optical spectrum again, only the excitations from the selected ground state are recorded. Unrelated absorptions in the optical spectrum will be eliminated. In Fig. 9(d) the spectrum cleared from the background by this so-called tagging method is shown.

3.2. ODMR Equipment

A schematic view on an absorption ODMR spectrometer is given in Fig.10. The sample to be investigated is enclosed in the cavity in a region of high microwave field

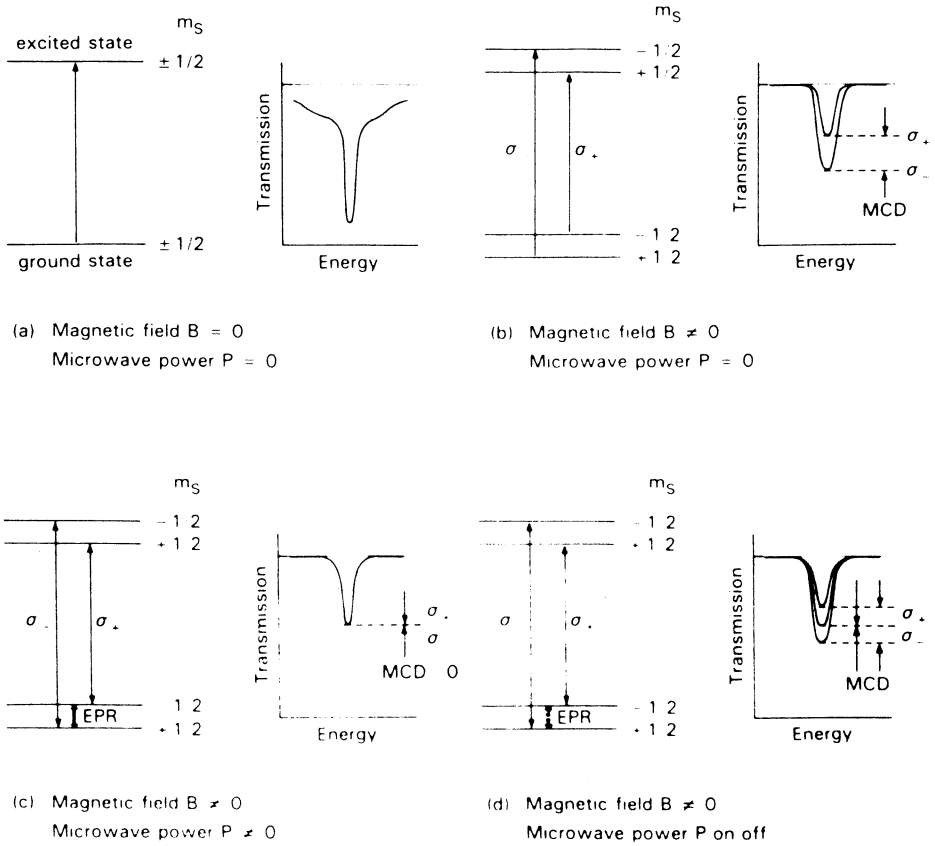

Figure 9 : Spectra of absorption ODMR. (a) Optical absorption spectrum, (b) MCD spectrum, (c) ODMR spectrum, (d) MCD spectrum tagged by EPR.

strength. The cavity must have openings to allow for the penetration of light for the optical absorption experiment. The very different wavelengths of the radiation involved allows the construction of cavities open to light but closed to microwaves. The optical path has a light source, a monochromator, a polarizer and detector. To enhance sensitivity and enable selectivity the microwave power and the sense of polarization of the light can be modulated at high speed. The signals are detected phase-sensitively by lock-in amplifiers.

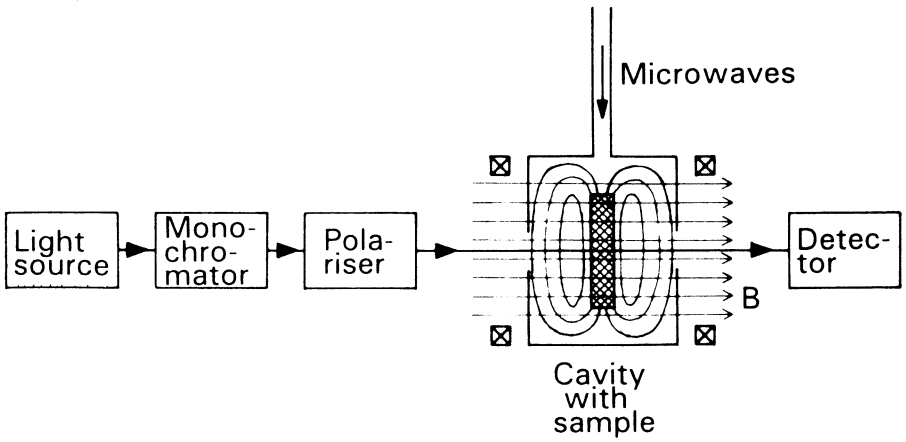

Figure 10 : Schematic of the experimental setup for an absorption ODMR spectrometer.

3.3. ODEPR of GaAs:EL2^{+}

An example following closely the discussion of basic concepts (in section 3.1) is provided by the EL2 centre in gallium arsenide [13]. The defect is a double donor and is paramagnetic in the ionized state $EL2^{+}$. An optical absorption spectrum below the bandgap energy is shown in Fig.11(a). Any structure in this spectrum is hard to distinguish. The magnetic circular dichroism as recorded for this absorption is shown in Fig.11(b). Since MCD is restricted to absorptions of defects with paramagnetic ground states the background is reduced considerably; for instance the sharp rise at the intrinsic band edge is eliminated. The MCD effect is small but the spectral structure in it is enhanced. This allows to establish more clearly the relation to other experiments yielding information on bandgap levels. The effect of magnetic resonance on the MCD at the wavelength $\lambda = 1.35$ μm gives the result of Fig.11(c). As usual, in this experiment the microwave frequency is kept constant at the cavity frequency, 24 GHz in this case, and the magnetic field is scanned to satisfy the resonance condition. The quartet of lines of equal intensity and equal spacing reflects resolved hyperfine interaction with one nucleus with spin $I = 3/2$ and 100% natural abundance. This reveals arsenic as a prominent constituent of the centre. Due to the selectivity the signal-to-noise ratio is remarkably high. Analysis of the isotropic spectrum yields g-value $g = 2.041$ and hyperfine interaction constant $A = 2670$ MHz, which identifies the centre as a previously reported As_{Ga} antisite related defect [14]. The electron paramagnetic resonance of this centre directly measured in EPR, near 35 GHz microwave frequency, is shown to demonstrate the similarity in Fig.11(d). Application of the microwaves at resonant conditions for a specific transition selects a specific ground

state of an optical transition for which the MCD is reduced. Scanning under such conditions over the optical energy range will then only show the optical excitations from the ground state for this selected centre. This tagging of optical excitation by EPR selects from the whole optical spectrum the part related to the EPR identified centre. For the GaAs:EL2 defect the EPR-tagged spectrum is shown in Fig.11(e). From the result one concludes that all transitions as observed in the MCD spectrum (Fig.11(b)) belong to the same centre.

3.4. ODENDOR Absorption Spectroscopy

In the mechanism invoked to explain ODMR the occupation of levels is a crucial factor. The induction of EPR allows the change of occupations of levels with different electron spin quantum numbers. In a similar way levels for different nuclear spin states can be influenced by nuclear magnetic resonance. For further specific explanation reference is made to Fig.12, which shows levels for an electron-nuclear spin system S = 1/2, I = 1/2. The difference between the electronic m_S = -1/2 levels and the m_S = +1/2 levels is given by the electronic Boltzmann ratio $\exp(g\mu_B B/kT)$. For instance for magnetic field B = 1T, temperature T = 1K, g = 2, S = 1/2, the population ratio will be near a

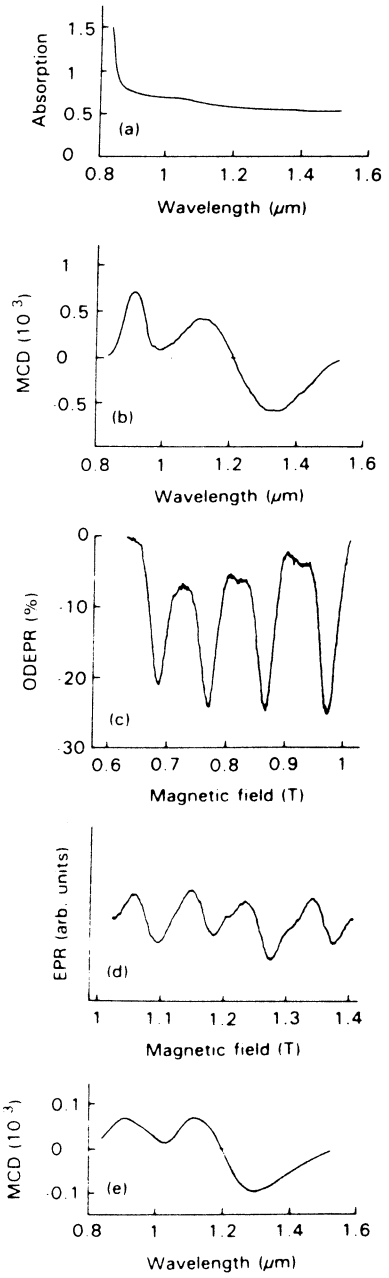

Figure 11 : Spectra of GaAs:EL2$^+$. (a) Optical absorption at 1.4 K (Ref. 13), (b) magnetic circular dichroism of the absorption for magnetic field B = 2 T (Ref. 13), (c) ODEPR at optical wavelength 1.35 μm and microwave frequency 24.31 GHz (Ref. 13), (d) electron paramagnetic resonance at 34.85 GHz (Ref. 14), (e) optical absorption tagged by spin resonance (Ref. 13).

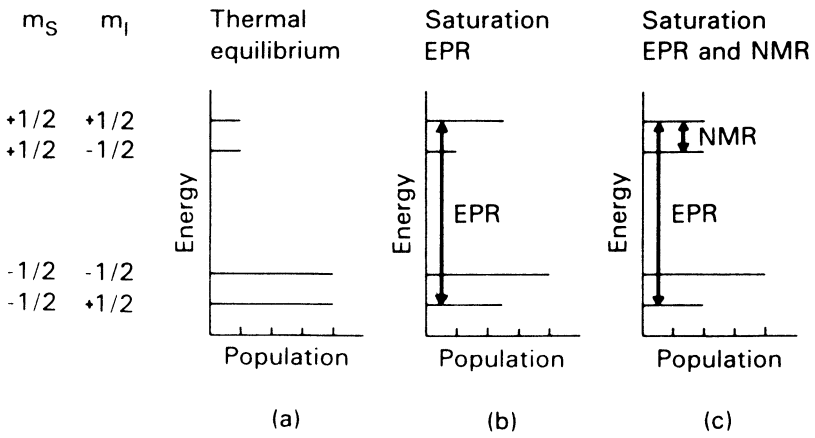

Figure 12 : Schematic to explain ODENDOR. (a) Levels and populations under thermal equilibrium ($B \approx 1T$, $T \approx 1K$) for the spin system $S = 1/2$, $I = 1/2$, (b) level populations with saturating EPR, (c) level populations with saturating EPR and NMR.

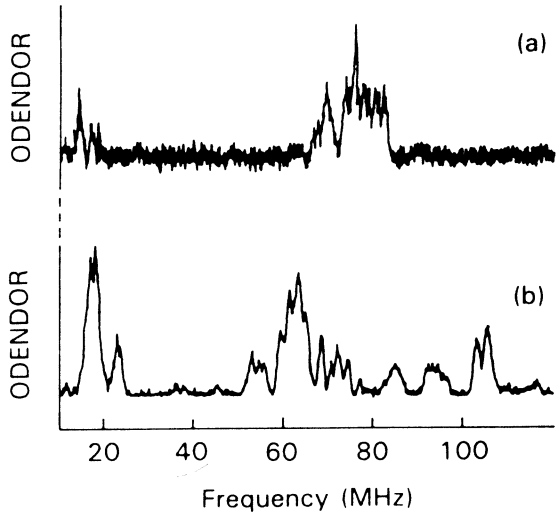

Figure 13 : ODENDOR spectra in GaAs for (a) the centre $EL2^+$ and (b) another As_{Ga} related defect, after Spaeth and Watkins[16].

factor 4. The small difference in occupation for different m_I values can be ignored. Selective saturation of the EPR transition for $m_I = +1/2$ equalizes the populations of the two connected levels (Fig.12(b)). The population difference of the two $m_S = -1/2$ levels with the two $m_S = +1/2$ levels is reduced to half of the original value. Application of saturation radio-frequency power for an NMR transition will further affect level populations as indicated in Fig.12(c). The MCD signal which is proportional to the occupation difference of $m_S = -1/2$ and $m_S = +1/2$ levels is again diminished. According to this description the effect of the NMR is of comparable magnitude to that of the EPR. The NMR measured via ODENDOR therefore experiences an even more dramatic enhancement of its sensitivity.

3.5. ODENDOR of GaAs:EL2$^+$

Measurements by EPR in III-V compounds, such as GaAs, suffer from appreciable linewidth broadening due to unresolved hyperfine interactions. The identification of defects in these materials on the basis of EPR parameters alone is in many cases inadequate. For instance, depending on sample treatment, there appear to be created many different defects related to the antisite structure As_{Ga}. Although these defects are different they are all characterized by g-value $g = 2.04 \pm 0.02$ and hyperfine interaction constant $A \approx 2650$ MHz. These centres can, however, have a different optical spectrum. Also ENDOR probes defect constituents and surroundings in a very sensitive manner. Defects with an indistinguishable EPR spectrum can be separated by their different ENDOR spectrum. In Fig.13 such results as measured by ODENDOR are illustrated for the EL2 defect and another As_{Ga} related defect in GaAs [15,16].

References

1. G. Schaefer, *J. Phys. Chem. Solids* **12** (1960) 233.
2. G.O. Jones, D.H. Martin, P.A. Mawer and C.H. Perry, *Proc. Roy. Soc.* (London) **A261** (1961) 10.
3. R.C. Newman and R.S. Smith, *J. Phys. Chem. Solids* **30** (1969) 1493.
4. L.V.C. Assali and J.R. Leite, *Phys. Rev. Lett.* **55** (1985) 980, **56** (1986) 403.
5. J.W. Corbett, S.J. Pearton and M. Stavola, in *"Defect Control in Semiconductors"*, ed. K. Sumino (Elsevier Science Publishers, Amsterdam, 1990), p. 53.
6. J.F. Angress, A.R. Goodwin and S.D. Smith, *Proc. Roy. Soc.* (London) **A287** (1965) 64.
7. W.G. Spitzer and M. Waldner, *J. Appl. Phys.* **36** (1965) 2450.
8. R.C. Newman and R.S. Smith, *Solid State Commun.* **5** (1967) 723.
9. R.S. Leigh and M.J.L. Sangster, *J. Phys.* **C15** (1982) L317.

10. R. Murray and R.C. Newman, in Landolt-Börnstein, New Series, Volume 22 *"Semiconductors", Subvolume b "Impurities and Defects in Group IV Elements and III-V Compounds"* (Springer, Berlin, 1989), p. 382.
11. H.J. Hrostowski and R.H. Kaiser, *Phys. Rev.* **107** (1957) 966.
12. R.C. Newman, in *"Defect Control in Semiconductors"*, ed. K. Sumino (Elsevier Science Publishers, Amsterdam, 1990), p. 65.
13. B.K. Meyer, J.-M. Spaeth and M. Scheffler, *Phys. Rev. Lett.* **52** (1984) 851.
14. R. Wörner, U. Kaufmann and J. Schneider, *Appl. Phys. Lett.* **40** (1982) 141.
15. J.-M. Spaeth, K. Krambrock and D.M. Hofmann, in *"The Physics of Semiconductors"*, eds. E.M. Anastassakis and J.D. Joannopoulos (World Scientific, Singapore, 1990), p. 441.
16. J.-M. Spaeth and G.D. Watkins, to be published in *"Submicroscopic Studies of Defects in Semiconductors"*, (North-Holland, Amsterdam, 1991).